International Journal of Electrical, Electronics and Computer Engineering **10**(1&2): 11-17(2021)

ISSN No. (Online): 2277-2626

A Dual Band Stacked Microstrip Patch Antenna with Monopolar Radiation Pattern for WLAN and V2X Communication

Suman Kumar Raj* and Ahmad Rafiquee

Department of Electronics and Communication Engineering,
Birla Institute of Technology, Mesra, Ranchi (Jharkhand) India.

(Corresponding author: Suman Kumar Raj)*
(Received 16 February 2021, Accepted 23 April 2021)
(Published by Research Trend, Website: www.researchtrend.net)

ABSTRACT: Adual-band, dual stacked microstrip patch antenna with Monopolar radiation pattern is proposed and analysed in this paper. An Annulus, TSAR and two sets of conductive vias are introduced into the structure to broaden the bandwidth and to drastically increase the antenna-gain. The realised impedance bandwidths are from 2.16 to 2.58 GHz in the low band and from 5.43 to 6.09 GHz in the high band, separately. The corresponding gains at low frequency band ranges from 7.1dBi to 7.8dBi and at high frequency band ranges from 8 to 9.7dBi. In addition, the proposed antenna has a low-profile structure, which can be easily placed on the top of a vehicle. In conjunction with these merits, the proposed design is very suitable for wireless local area network (2.4–2.48 GHz and 5.75–5.825 GHz), Satellite positioning system using S-band of NavIC (2483.50 – 2500.00MHz) and Vehicle to everything (5.85–5.925GHz) communications.

Keywords: Dual-band, V2X Communication, DSRC, Satellite positioning system (SPS), Indian Regional Navigation Satellite System (IRNSS).

INTRODUCTION

Connected and fully automated vehicles are likely to modernize future transportation systems around the globe. Vehicle-to-everything (V2X) communications have become increasingly prevalent around the globe, as the key facilitator of intelligent transportation systems (ITS) [1]. 5GAA mentioned the use cases for V2X in four Categories: Safety, Convenience, Advanced Driving assistance, Vehicle Platooning leading towards connected vehicles and autonomous driving [2, 4]. Currently there are two key technologies that facilitates V2X communication, capable of supporting aforesaid vehicular applications. These are Dedicated short-range communications (DSRC) based on IEEE 802.11p protocol and cellular-V2X (C-V2X) based on cellular technologies. DSRC was introduced more than a decade ago. DSRC fits for most of the vehicular applications set by ITS. Although it experienced serious limitations in dense environment and high mobility scenario (beyond 200km/hr) which led to delayed global adoption of DSRC [5].

Meanwhile in 2014, 3rd Generation Partnership Project (3GPP) introduced C-V2X in Rel.14 with similar set goals. A detail comparison of DSRC and C-V2X can be found in [6, 7].

In order to accommodate enhanced vehicular applications, DSRC and C-V2X, both are receiving considerable improvements. To overcome the above issue and improved use cases with backward compatibility, IEEE created a task force for evolution of 802.11p. This evolution is named as IEEE 802.11bd. Similarly, 3GPP introduced NR V2X in Rel.16.

The key objectives, detailed description and current enhancements of 802.11bd and NR V2X is discussed in [5-8]. One of the key objectives of 802.11bd /NR V2X is to offer accurate, real-time vehicle positioning. In order to achieve this, 802.11bd is expected to employ the positioning system. In context of Indian geographical region for conventional positioning, the Indian Regional Navigation Satellite System (IRNSS) often known as NavIC (Navigation with Indian Constellation) would be utilised [9]. It is mandatory for commercial cars in India to be equipped with NavIC [10, 11].

Antenna Design for V2X application is one of the major components to achieve the aforesaid goals set by ITS. In V2X Communications, the vehicles and Road side Units (RSU) are distributed in different directions. In order to establish communication link between vehicle to vehicle, vehicle to RSUs to carry out successful transmission and reception of data all the time, such antennas are desired which have quasi-omni directional like monopolar radiation patterns [12]. Recent years have seen exponential growth in wireless technologies, wireless local area network (WLAN), Standard Positioning System (SPS) and Vehicle-to-Vehicle (V2V) communications have been extensively used in vehicular communications for internet access, safe driving and traffic safety [13]. In Radio frequency spectrum, 2.4/5.8 GHz (IEEE 802.11a/b/g/n) bands are allocated for Wireless Local Area Network (WLAN), for NavIC system a band of 16.5 MHz is allocated in 2.49GHz [14] and for V2X communications from 5.85 to 5.925 GHz (IEEE 802.11p) band is allocated. Due to this(for WLAN and V2X communications), a dual-band antenna with quasi-omnidirectional like monopolar radiation patterns is essential to be mounted on the vehicle. The commercially available antennas for V2X

communication comprise antennas having omnidirectional pattern with gain around 6-6.5dBi and directional antennas with the gain of 12dBi [15]. Antennas with directive radiation patterns may also be used for V2X communication. However, they can't cover whole horizontal plane because they radiate in a specific direction. Varying the locations of these antennas on the vehicle could widely cover the horizontal plane at a cost of more antennas. The design and measurement of quasi-omnidirectional or monopolar radiation pattern antennas for V2X communication can easily be found in literature [15-18].

In past, various kind of antennas has been used for establishing link between Vehicle to Vehicle (V2V), Vehicle to Infrastructure (V2I), Vehicle to pedestrian (V2P). The Microstrip patch antennas are popular for low profile applications and has a planar structure.

In this Paper, a low-profile dual-band stacked microstrip patch antenna having monopolar radiation pattern is proposed. By utilising a stacked patch structure, the antenna can operate at two frequency bands. It can offer a dual-band operation in 2.16-2.58 GHz and 5.43-6.09 GHz band. By adding a coupled annulus and two distinct sets of conductive vias to the antenna arrangement improves the antenna bandwidth and gain dramatically. A detailed Antenna Configuration and antenna geometry can be found in section II. In Section III antenna analysis is done. Section IV presents the results and discussion. Finally, Section V discusses the conclusion.

II. ANTENNA GEOMETRY

The geometry of the proposed antenna is depicted in Fig. 1, and the specific dimensions of various parameters are listed in Table 1.

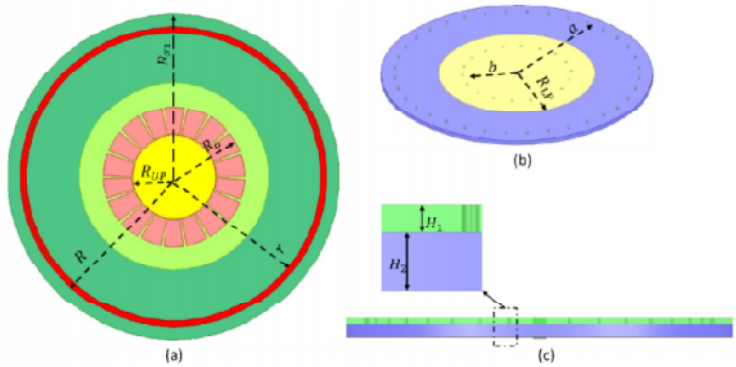

Fig. 1. (a) detailed structure of antenna Geometry, (a) Top View, (b) Isometric view of lower Patch, (c) Side view.

Table 1: Dimensions of proposed Antenna.

Antenna Parameters	R_{S1}	R_{S2}	R_g	R_{LP}	R_{UP}	R_{via1}	R_{via2}	R	r	H_1	H_2	R_o
Values (in mm)	80	80	80	46	20.5	0.6	0.6	74	71	1.5	3.175	34.5

The proposed antenna has stacked structure. The antenna mainly comprises of a ground plane, two substrates (Substrate 1 & 2), a lower circular patch, an upper circular patch, an annulus, a trapezoidal shaped angular ring (TSAR), two sets of conductive vias (one set is in the lower patch and another set is in the annulus) and coaxial probe. The ground plane has a radius of R_g and is located at the bottom most section of the structure. Substrate 1 is stacked on the top of Substrate 2. The material used for Substrate 1 is Arlon AD260A with a relative permittivity of 2.6 while Substrate 2 is made of Rogers 5870, which has a relative permittivity of 2.33. H_1 and H_2 are the thickness of two substrates, respectively. The upper circular patch having radius R_{UP} is on the top of Substrate 1 while on the top of Substrate 2, the lower circular patch with a radius of R_{LP} is placed.

The annulus on the top of Substrate 1 has an outside radius of R and an interior radius of r. To short with ground, a series of 36 Conductive Vias are placed inside the annulus. Each via has a radius of R_{via2}. Vias is surrounded in the middle of the annulus which is "a=72 mm" away from the centre of the antenna geometry.

The lower circular patch has 18 conducting vias placed into it. These 18 conductive vias are loaded symmetrically about the feed location, shorting the lower circular patch. The Radius of each via is R_{via1} and the centre of each via is "b= 32 mm" distant from the centre of the lower circular patch. A coaxial probe with a typical impedance of 50 ohm is used to feed the antenna. To generate the Zeroth order resonance (ZOR) mode, the inner conductor travels through a clearance hole from the centre of the lower circular patch, which immediately joins the centre of the higher circular patch.

A circular patch antenna can be considered a cylindrical cavity with respect to the free-space wavelength λ_0, if the substrate thickness is extremely small, a circular patch antenna can be considered as a cylindrical cavity [13]. The TM_{mn} mode inside the antennacan then be studied using a cavity model. In terms of [19-22] the effective radius a_{eff}, of the circular patch and the resonant frequency f_{mn} of the antenna can be calculated as follows:

Table 2: Values for x_{mn}.

n/m	0	1	2	3	4	5
1	3.832	1.841	3.054	4.201	5.317	5.416
2	7.016	5.331	6.706	8.015	9.282	10.520
3	10.173	8.536	9.969	11.346	12.682	13.987

$$f_{mn} = \frac{c}{2\pi a\sqrt{\varepsilon_r}} x_{mn} \quad (1)$$

$$a_{eff} = a\sqrt{1 + \frac{2h}{\pi a \varepsilon_r}\left(\ln\frac{\pi a}{2h} + 1.7726\right)} \quad (2)$$

$x_{mn} = ka_{eff}$

x_{mn} = nth zero of the derivatives of the Bessel's function of order m.

c= speed of light in the free space.

a = radius of the patch.

ε_r = Dielectric constant.

III. ANALYSIS

Our design approach is to simultaneously excite and combine several TM_{0n} resonance modes, for obtaining monopole-like radiation pattern, till the desired frequency band and Gain according to the V2X application is achieved.

In general, TM_{0n} modes produce better omnidirectional pattern particularly in the azimuth plane, with a better gain compared to another modes (e.g., TM_{21}, TM_{31}, TM_{41}) excited [21, 25].

To analyse the different modes, we have plotted Current density (J Surf- vector) at resonating frequencies 2.25GHz, 2.45 GHz, 5.45 GHz, 6 GHz which clearly signifies the different modes at these frequencies. The plot of Current densities at afore-mentioned frequencies can be found in Fig. 3.

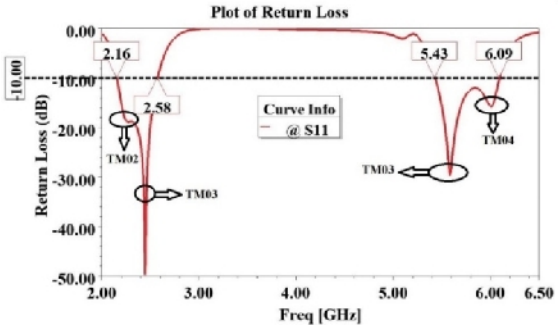

Fig. 2. S11 Parameter along with Generated modes.

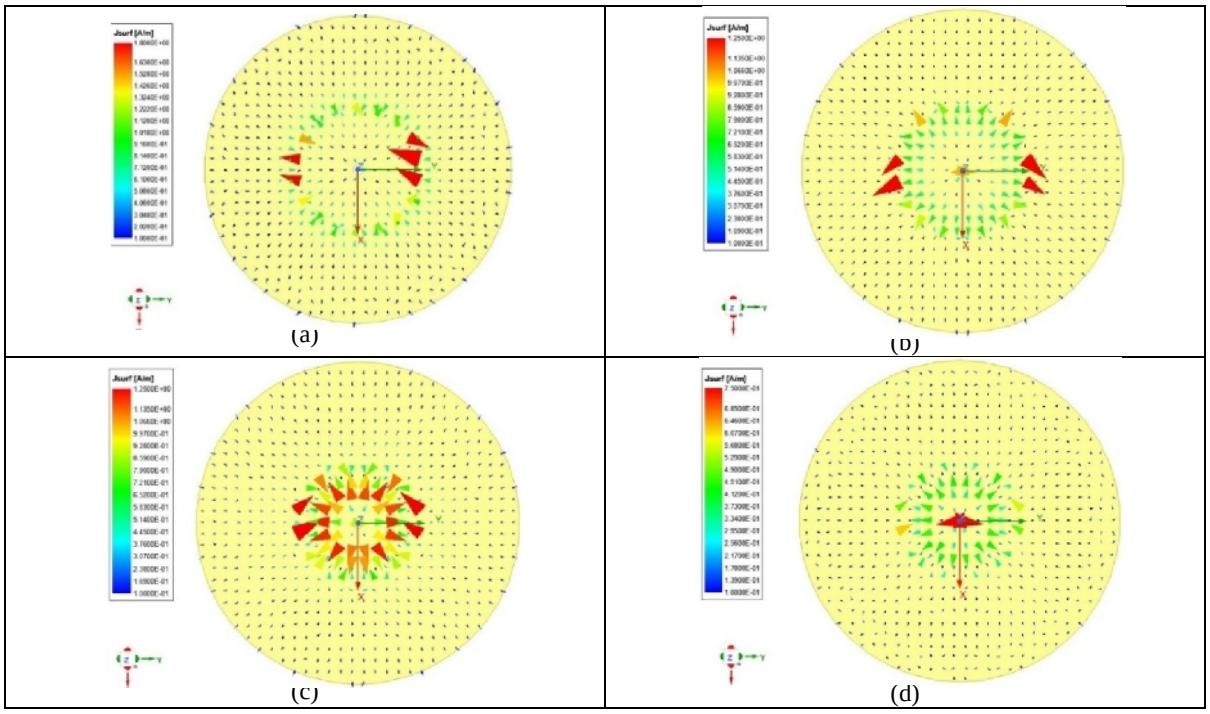

Fig. 3. Current density (J Surf- vector) at resonating frequencies (a) 2.25GHz, (b) 2.45 GHz, (c) 5.45 GHz, (d) 6 GHz.

Conductive Vias in lower patch. To produce a large bandwidth in the low band, a series of conductive vias are placed into the antenna structure, shorting the lower circular patch with the ground plane. The conductive vias in the lower patch generates another mode and after optimization of the patch size and the distance of vias from the feed point a wide bandwidth has been achieved starting from 2.16 GHz to 2.58 GHz. From the Fig. 3 it can be found that TM_{02} mode and TM_{03} is generated at 2.25 GHz and 2.45 GHz which is lower resonant frequency and the higher resonant frequency of lower band respectively. The vias in lower patch also effects higher band of antenna. A detailed analysis of conductive vias in lower patch is mentioned in Table 2.

Table 2: Detailed Analysis of Conductive Vias in Lower Patch.

Sr. No.	Antenna Structure	Bandwidth (in GHz)	
		Lower Band	Upper Band
1.	Antenna without Vias in Lower Patch	2.53-2.58	5.99-6.12
2.	Antenna with 4 Vias in Lower Patch	2.52-2.59	5.99-6.16
3.	Antenna with 8 Vias in Lower Patch	2.49-2.59	5.96-6.13
4.	Antenna with 18 Vias in Lower Patch	2.16-2.58	5.43-6.09

A trapezoidal shaped angular ring. When a coupled trapezoidal shaped angular ring is incorporated with upper circular patch, the impedance bandwidth in the upper frequency band is considerably widened. Fig. 4 illustrates the simulated return loss (S11) with and without the TSAR in the upper frequency band. If a trapezoidal shaped angular ring is added to the antenna, the antenna bandwidth increases by 12% from 5.43 to 6.09 GHz in the high band, as shown in the diagram. However, when the TSAR is eliminated from the antenna geometry, there is an impedance miss-match and is impossible to get a good matching. Thus, the reflection coefficients rise above −10 dB.

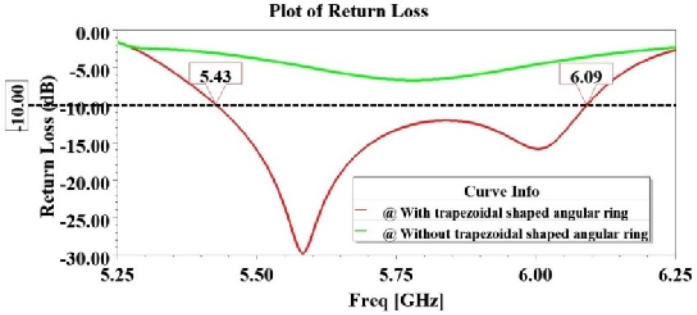

Fig. 4. Comparison of S11 parameter with TSAR and without TSAR at upper frequency band.

Simulated surface current distributions on the upper circular patch and the TSAR at 5.5 and 6 GHz are displayed in Fig. 5. Further demonstrating the TSAR's working mechanism. Comparing the currents on the TSAR to those at 5.5 GHz, the currents on the 6 GHz ring are stronger, showing that at this frequency the ring acts as a radiator. As a result, a broad bandwidth can be achieved in the upper frequency band when the TSAR is incorporated with the upper circular patch. This also results the generation of additional TM_{04} mode, which can be seen from Fig. 5.

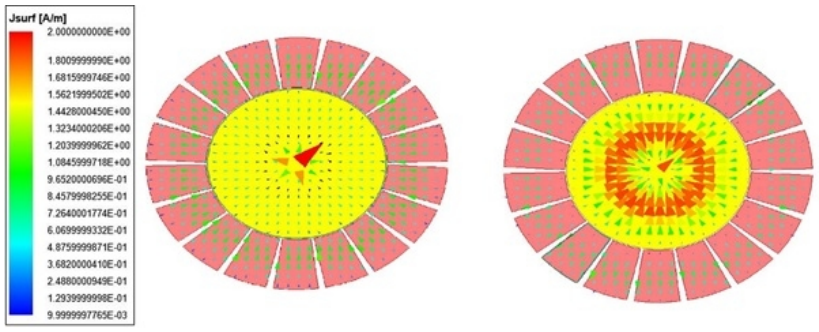

(a) Current density at 5.5 GHz (b) Current density at 6 GHz

Fig. 5. Current density (J Surf- vector) on TSAR Surface at higher band.

Annulus. Further by inserting annulus to the structure and optimising the placement of annulus by keeping the centre of structure as reference and shorting annulus through set of vias with the ground, we observe increment in gain at high band. A detailed analysis of Gain with shorted annulus and without annulus is tabulated in Table 3.

Table 3: Detailed Analysis of Conductive Vias in Lower Patch.

Sr. No.	Antenna Structure	Gain (in dBi)					
		2.16 GHz	2.58 GHz	5.43 GHz	5.85 GHz	5.925 GHz	6.09 GHz
1.	Antenna with 36 Vias in Annulus	7.1	7.8	8	8.4	8.6	9.7
2.	Antenna without Annulus	7.1	8	6.3	7.7	8.25	9.3
3.	Antenna with 5 Vias in Annulus	7	7.97	6.7	7.38	7.94	9.03
4.	Antenna with 9 Vias in Annulus	7	8	6.4	8	8.3	9.3
5.	Antenna with 18 Vias in Annulus	7.1	7.9	6.49	7.6	8	9.19
6.	Antenna with Annulus only	7.2	7.9	6.5	7.5	8.1	9.3

IV. RESULTS AND DISCUSSION

The proposed dual band microstrip patch antenna is designed and simulated on Ansys HFSS using the design parameters given above in section II. The operating frequency bands for the proposed antenna ranges from 2.16 GHz to 2.58 GHz and from 5.43 GHz to 6.09 GHz which covers WLAN, NavIC and V2X Communication bands. The return loss (S11) of the proposed antenna is given in Fig. 2. The simulated return loss is below -10dB in both the operating frequency bands. The corresponding gains at low frequency band ranges from 7.1dBi to 7.8dBi and at high frequency band ranges from 8 to 9.7dBi. The 3D-Gain plot (dBi) for the proposed antenna at four resonant frequencies i.e. 2.25, 2.45, 5.58 and 6GHz are shown in Fig .6.

From Fig. 6 it can be seen that value of gain at these resonant frequencies are 7.4 dBi, 7.8 dBi, 8.0 dBi and 9.0 dBi respectively. Due to different modes generated, the radiation patterns are different. The radiation pattern at all the resonating frequencies is quasi-omnidirectional which can be clearly observed from the 2D radiation pattern figured in Fig. 7.

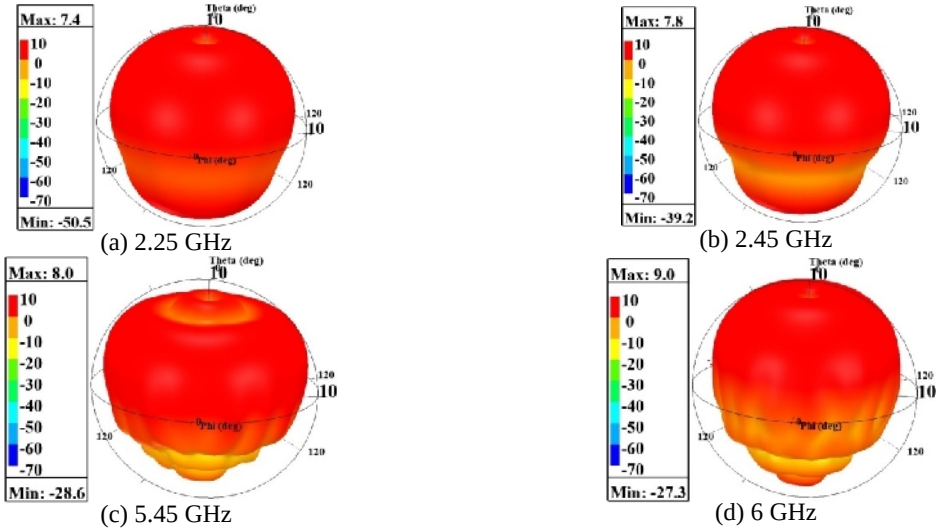

(a) 2.25 GHz (b) 2.45 GHz (c) 5.45 GHz (d) 6 GHz

Fig. 6. 3D-Gain plot.

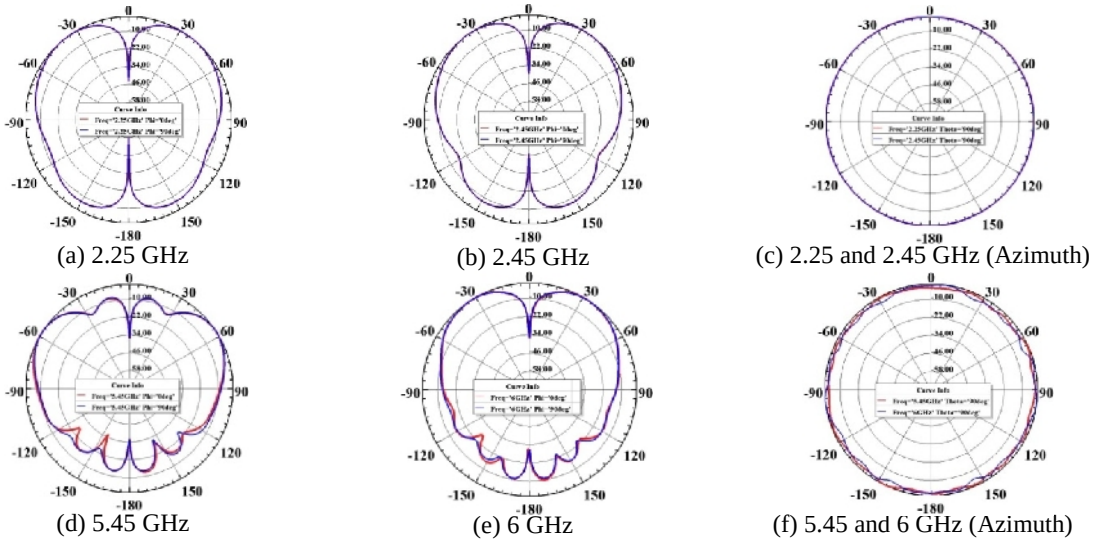

(a) 2.25 GHz (b) 2.45 GHz (c) 2.25 and 2.45 GHz (Azimuth)

(d) 5.45 GHz (e) 6 GHz (f) 5.45 and 6 GHz (Azimuth)

Fig. 7. Far-field radiation patterns.

The proposed antenna is having monopole radiation pattern in lower as well as in higher band. The maximum radiation of antenna is mainly at $\theta = 60^{\circ} \pm 50^{\circ}$ in elevation plane for both i.e. $\phi = 0^{\circ}$ and 90° respectively, while in azimuth plane the antenna is having almost uniform radiation pattern. For V2X communication it is very important that car or vehicles can cover complete horizontal plane while in vertical plane the gain value should reduce. So, depending upon the application the proposed antenna's far-field radiation patterns at 2.4 GHz, 5.85 GHz, 5.95 GHz frequencies are shown in Fig. 8 and 9 respectively.

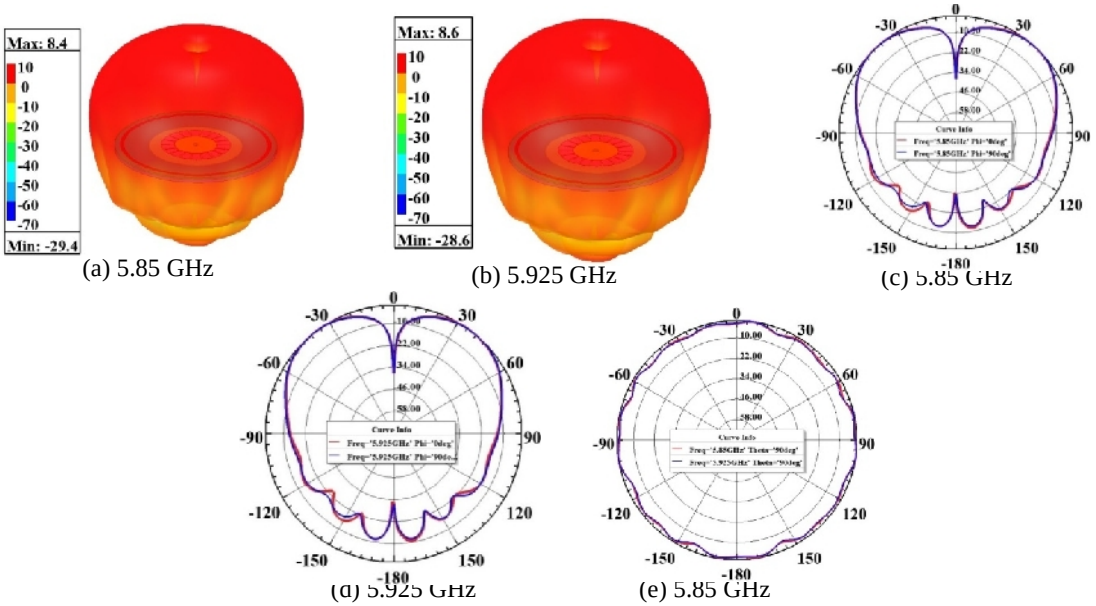

(a) 5.85 GHz (b) 5.925 GHz (c) 5.85 GHz

(d) 5.925 GHz (e) 5.85 GHz

Fig. 8. 3D Gain plot with proposed antenna and 2D Radiation pattern at V2X Operating band.

For the V2X communications, the placement of antenna is critical. The proposed antenna can be placed at the roof of the vehicle. At the operating band of V2X communication, the antenna has a null for the $\theta = 0^{\circ}$ and the main beam is around $\pm 30^{\circ}$ to $\pm 45^{\circ}$ in elevation plane of antenna and the 3-dB beamwidth of the antenna is almost 45°. In azimuth plane, the antenna has almost uniform radiation.

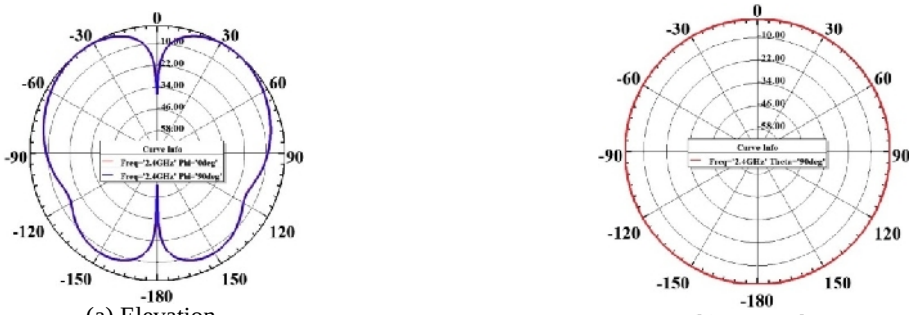

(a) Elevation (b) Azimuth

Fig. 9. 2D Radiation pattern for WLAN.

Our proposed antenna is showing good characteristics for all the above application as its beam will cover the maximum no of RSU, and the antenna has full coverage in the azimuth plane as shown in Fig. 8 and 9. Therefore, this type of radiation pattern is most desirable for V2V, V2I, V2N and V2P.

CONCLUSION

Adual bandstacked microstrip patch antenna with monopolar radiation pattern for WLAN and V2X communication has been presented in this paper. The designed antenna covers Wi-Fi 2.4/5GHz band, INRSS S-Band and V2X frequency bands. Over two bands, simulation results show that omnidirectional radiation patterns can be generated. Furthermore, the antenna has a low-profile design. Altogether, the proposed design is suitable for WLAN and V2X communications.

REFERENCES

[1]. Yuan, W., Li, S., Xiang, L., and Ng, D. W. K. (2020). Distributed estimation framework for beyond 5G intelligent vehicular networks. *IEEE Open Journal of Vehicular Technology*, **1**, 190-214.

[2]. Boban, M., Kousaridas, A., Manolakis, K., Eichinger, J., and Xu, W. (2018). Connected roads of the future: Use cases, requirements, and design considerations for vehicle-to-everything communications. *IEEE vehicular technology magazine*, **13**(3): 110-123.

[3]. Masini, B. M., Silva, C. M., and Balador, A. (2020). The use of meta-surfaces in vehicular networks. *Journal of Sensor and Actuator Networks*, **9**(1): 15.
[4]. White Paper, 5GAA Automotive Association T-200043 (2020). "C-V2X Use Cases Volume II: Examples and Service Level Requirements".
[5]. Naik, G., Choudhury, B. and Park, J. (2019). "IEEE 802.11bd & 5G NR V2X: Evolution of Radio Access Technologies for V2X Communications," in *IEEE Access*, **7**, pp. 70169-70184.
[6]. [Online]. Sean Conway(Sep. 2018), 5GAA.V2X Technology Benchmark Testing.
[7]. Shrestha, R., Nam, S. Y., Bajracharya, R. and Kim, S. (2020). "Evolution of V2X Communication and Integration of Blockchain for Security Enhancements". *Electronics*, **9**(9), 1338.
[8]. [Online]. 3GPP Rel.16: ETSI Work Programme report (2019). [Accessed on 27th May 2021]. Available: http://www.3gpp.org/release-16
[9]. "IRNSS-1G exemplifies 'Make in India', says PM". The Statesman. (28 April 2016), Archived from the original on 23 September 2016.
[10]. "Government of India, Ministry of Space, Lok Sabha - Unstarred Question number: 483 on Progress of IRNSS", (20 November 2019). Archived from the original on 17 February 2020.
[11]. "Government of India, Ministry of Space, Lok Sabha, Unstarred Question No: 675 on Indigenous GPS"(26 June 2019), Archivedfrom the original on 17 February 2020. Retrieved 17 February 2020, Accessed on 7th June 2021.
[12]. Neira, Edith Condo (2017). *Antenna evaluation for vehicular applications in multipath environment*. PhD Thesis, Diss. Chalmers Tekniska Hogskola (Sweden).
[13]. Gao, S., Ge, L. Zhang, D. and Qin, W. (2018), "Low-Profile Dual-Band Stacked Microstrip Monopolar Patch Antenna for WLAN and Car-to-Car Communications", in *IEEE Access*, **6**, pp. 69575-69581.
[14]. "IRNSS Signal in space ICD for standard positioning service", version 1.1, ISRO SatelliteCentre Bangalore, August 2017. Available: Link
[15]. Abishek, E. B., Raja, A. V. P., Kumar, K. P. C., Stephen, A. C., and Raaza, A. (2017). Study and analysis of conformal antennas for vehicular communication applications. *ARPN Journal of Engineering and Applied Sciences*, **12**, 2428-2433.
[16]. Abbas, T., Karedal, J. and Tufvesson, F. (2013). "Measurement-Based Analysis: The Effect of Complementary Antennas and Diversity on Vehicle-to-Vehicle Communication", in *IEEE Antennas and Wireless Propagation Letters*, **12**, pp. 309-312.
[17]. Gallo, M., Bruni, S., Pannozzo, M. and Zamberlan, D. (2013). "Performance evaluation of C2C antennas on car body" (2013). *2013 7th European Conference on Antennas and Propagation (EuCAP)*, pp. 3136-3139.
[18]. Kaul, S. and Ramachandran, K. and Shankar, P. and Oh, S., Gruteser, M., Seskar, I. and Nadeem, T. (2007). "Effect of antenna placement and diversity on vehicular network communications", *2007 4th Annual IEEE Communications Society Conference on Sensor, Mesh and Ad Hoc Communications and Networks*.
[19]. Balanis, Constantine A. (2015). *Antenna theory: analysis and design 2nd ed*. John wiley & sons.
[20]. Bancroft, R. (2019). *Microstrip and printed antenna design 2nd ed*. Institution of Engineering and Technology.
[21]. Garg, R., Bhartia, P., Bahl, I. J. and Ittipiboon (2001). A. *Microstrip antenna design handbook*. Artech house.
[22]. Shen, L., Long, S., Allerding, M. and Walton, M. (1977). "Resonant frequency of a circular disc, printed-circuit antenna," in *IEEE Transactions on Antennas and Propagation*, **25**(4), 595-596.
[23]. Garg, R., Bhartia, R., Bahl, I. and Ittipiboon, A. (2001). "Circular disk and ring antennas", in *Microstrip Antenna Design Handbook*. Boston: Artech House, Inc., ch. 5, pp. 317–398.
[24]. Tak, J., and Choi, J. (2014). Circular-ring patch antenna with higher order mode for on-body communications. *Microwave and Optical Technology Letters*, **56**(7), 1543-1547.
[25]. Liu, S., Wu, W., and Fang, D. G. (2016). Wideband monopole-like radiation pattern circular patch antenna with high gain and low cross-polarization. *IEEE Transactions on Antennas and Propagation*, **64**(5), 2042-2045.